
ORIGINAL ARTICLE

Ultrastructural Changes in Axons Following Exposure to Pulsed Radiofrequency Fields

Serdar Erdine, MD^{*}; Ayhan Bilir, MD[†]; Eric R. Cosman Sr., PhD[§];
Eric R. Cosman Jr., PhD[¶]

^{}Department of Algology, Istanbul Faculty of Medicine, Istanbul University, Capa Kinikleri, Cerrahi Monoblok, Istanbul; [†]Department of Histology and Embryology, Faculty of Medicine, Istanbul University, Cap, Istanbul, Turkey; [§]Department of Physics, Massachusetts Institute of Technology, Cambridge, Massachusetts; [¶]Cosman Medical, Inc., Burlington, Massachusetts, U.S.A.*

■ **Abstract:** Pulsed radiofrequency (PRF) fields applied by an electrode to neural structures, such as the peripheral sensory nociceptor axons and dorsal root ganglion, are clinically effective in reducing pain and other neuropathic syndromes. However, a full understanding of the underlying mechanisms by which this occurs has not yet been clarified. In this study, PRF is applied to the afferent axons of the sciatic nerves of rats. A standard radiofrequency (RF) electrode and RF generator is used to apply the RF signal output to the sciatic nerve using standard PRF parameters that have been successfully used in clinical practice. The ultrastructure of the treated axons is observed after 10 days by electron microscopy. A control, sham application is simultaneously applied to the contralateral sciatic nerve to provide a statistical differential comparison. It is found that the internal ultrastructural components of the axons show microscopic damage after PRF exposure, including: abnormal membranes and morphology of mitochondria, and disruption and disorganization of microfilaments and microtubules. The damage appears to be more pronounced for C-fibers than for

A-delta and A-beta fibers. The results are discussed in terms of internal electric field strengths and thermodynamic parameters. ■

Key Words: pulsed radiofrequency, PRF, sensory axon, electron microscopy, microtubules, mitochondria

INTRODUCTION

The pulsed radiofrequency (PRF) technique has been effective in the treatment of numerous pain and neuropathic syndromes. Like the classical continuous radiofrequency (CRF) technique, it involves the placement of a radiofrequency (RF) electrode in proximity to the neural target structure and delivery of an RF signal output from an RF generator to that structure. The difference is that in CRF, the signal output is typically a continuous wave of RF voltage (and therefore a continuous wave of RF current), whereas in PRF, the RF wave is broken up into short bursts of signal output between which are time periods of no signal at all. In the typical CRF technique, the tissue is heated grossly by electrical energy dissipation, and it is the tissue heating that leads to localized destruction of the neural tissue and consequent interruption of neural signaling. This has historically been called the RF heat lesion. The

Address correspondence and reprint requests to: Eric R. Cosman Jr., PhD, 872 Concord Avenue, Belmont, MA 02478, U.S.A. E-mail: ercosman@mit.edu.

Submitted: June 29, 2009; Accepted: July 18, 2009
DOI: 10.1111/j.1533-2500.2009.00317.x

typical PRF technique is characterized by much lower average temperature elevations of the target tissue because of the smaller duty cycle on time of the PRF pulsatory RF output. Indeed, PRF is often effective without raising the average target tissue temperature above 42°C, which has been traditionally been thought to be below the irreversible tissue destruction threshold (ie, the heat-lesion threshold) of 45°C to 50°C.

Since its discovery,¹ it has been speculated that PRF is a modulatory or nondestructive technique. However, this has not been proven, and some evidence to the contrary has been shown.^{2,3} The perception that PRF is nondestructive is encouraged by the following factors: (1) PRF can be effective for tissue temperatures below the heat-lesion threshold, (2) in most cases, there is no significant sensory loss following PRF, and (3) there is often imperceptible discomfort during a PRF treatment, even near highly sensitive structures such as the dorsal root ganglion (DRG), for which a CRF treatment can be intolerably painful. On the other hand, it has been shown by electron microscopy² that there is significant disruption of the ultrastructure in the soma of neurons in the DRG that has been exposed to PRF. Another study³ has shown that when neurons are subjected to the abnormally high electric fields characteristic of PRF, those neurons are subjected to large transmembrane potentials and localized heat flashes whose temperatures exceed the heat-lesion threshold; both of these could have a destructive effect on the neurons, on either a macroscopic or microscope scale.

In this article, the structural effects of PRF on sensory nociceptive axons are studied using electron microscopy. It has been reported⁴ that PRF is clinically effective at relieving pain when applied to pure afferent sensory nerves such as the medial branch for the treatment of facet-related pain. An objective of this study is to determine experimentally if there is a physical change in the gross structure or the ultrastructure of axons after PRF that might account for these clinical observations. The effect on axons was chosen rather than the soma of the DRG, because the ultrastructure in the axons is less complex than in the soma, and thus the interpretation of results may be clearer. This will potentially enable physical modeling of the interaction of electric forces on cellular structures, which could provide an explanation for the pain-relieving phenomenon of PRF.³

METHODS AND MATERIALS

The PRF study was performed on the sciatic nerves of five male Wistar Albino rats, weighing 220 to 250 g. All

rats were housed in a quiet and temperature-controlled room ($21 \pm 3^\circ\text{C}$), maintained on a 12-hour light/dark cycle (0700 to 1900), and were allowed food and water *ad libitum*. All procedures were approved by the Experimental Animal and Research Ethical Committee. The animals were acclimatized to laboratory for at least 1 hour before testing, and the experiments were performed in accordance with current guidelines for the care of laboratory animals and ethical guidelines for investigations of experimental pain in conscious animals.⁵

Surgical Electrode Positioning

The procedure was performed using ketamine anesthesia (35 mg/kg). A surgical incision above the sciatic nerve of minimal length allowed exact positioning of the electrode tip in contact with the nerve as shown in Figure 1. Once the electrode was positioned, the incision was closed tightly around the electrode; this was sufficient to stabilize the position of the cannula in the tissue and against the sciatic nerve. The goal was to have the tissue surrounding the nerve and electrode in the same configuration as it would have been if the electrode had been perfectly placed percutaneously, as it is in the clinical context. The sharpened portion of the tip of the electrode was placed deep enough so that only the cylindrical wall of the electrode was in contact with the epineurium. Therefore, the exposed metal tip of the RF electrode was positioned so the cylindrical side wall of the electrode was in contact with the sciatic nerve, not the sharpened point or the sharp bevel edges of the electrode tip. This was done because the electric field at the cylindrical “side barrel” of the electrode is very well defined compared to singularities at the sharp edges near the bevel point,³ for which the change of field strength as a function from distance for the electrode is very rapid and less definable. Thus, a quantitative analysis of any structural effects seen in the experimental configuration can be better interpreted with respect to the magnitude of the electric fields on the axons of the sciatic nerve. Furthermore, this configuration has been used clinically on the medial branch PRF exposures, so that any observed effects would be relevant to the question of the origin of pain relief for PRF.

Radiofrequency Equipment

The RF generator was a Cosman RFG-1B RF Generator (Cosman Medical, Inc., Burlington, MA, USA), and the electrode system was a standard Cosman CC-C5422 RF cannula into which was inserted a Cosman CSK-TC5

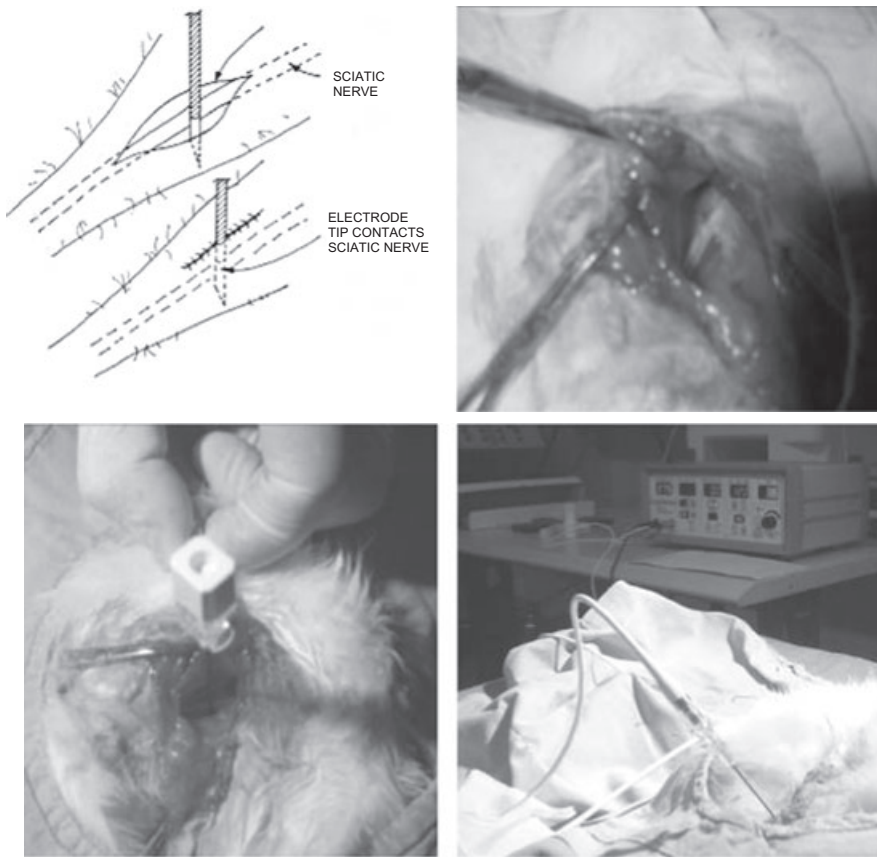


Figure 1. (Upper left) Placement of the side of the exposed Cosman CC-C5422 cannula tip against the sciatic nerve, and the suturing of the cannula shaft to fix its position. (Upper right) Surgical exposure of the sciatic nerve. (Lower left) Inserting the CC cannula in place adjacent to the sciatic nerve. (Lower right) Creating the pulsed radiofrequency exposure with the Cosman CSK-TC Electrode placed in the CC cannula and connected to the Cosman RFG-1B RF Generator.

thermocouple temperature monitoring electrode. This type of cannulae is used clinically for PRF procedures in the cervical and lumbar spine, and it has a 4-mm-long exposed electrode tip, a 5-cm shaft length, and a 0.7-mm (22 gauge) shaft diameter. The cannula tip has a sharpened beveled point, normally used for percutaneous insertion, but in this experiment the sharp bevel was not in contact with the sciatic nerve of the rat.

Standard clinical PRF parameters were used for the sciatic nerve exposure. These are: Voltage = 45 V, Pulse Width = 20 milliseconds, Pulse Rate = 2 Hz (pulses per second). As is common clinical practice, the average temperature of electrode tip, as measured by the Cosman CSK-TC electrode, was never allowed to go above 42°C, by reducing the RF voltage from the 45 V level as necessary.

Experimental Method and Microscopic Analysis

For each of the rats, the PRF was applied to the left side sciatic nerve. The right side sciatic nerve was used as a sham control in which an identical RF electrode was positioned against the sciatic nerve and closed over exactly as on the left side, but no PRF exposure was

done. In both the left- and right-side procedures, the incisions were closed, layer-to-layer, with 3-0 silk sutures. The rats were allowed to recover from the anesthesia. After surgery, the animals were individually maintained in plastic cages with solid floors covered with sawdust. All animals postoperatively displayed normal feeding and drinking behavior. At the end of 10 days, no neurologic deficits on the lower extremities were observed on either side.

Ten days after surgery, sciatic nerves both from PRF side (left) and sham side (right) were removed. Tissue samples of 1 mm³ were fixed with 2.5% glutaraldehyde in 0.1 M sodium cacodylate buffer, and postfixed in 1% osmium tetroxide in 0.1 M sodium cacodylate buffer for 1 hour at 4°C. Tissues were incubated in 1% uranyl acetate for 1 hour at 4°C. Passive fixation was allowed at 4°C for 1 hour in 1% osmium tetroxide and 0.1 molar cacodylate buffer. Tissues were incubated in 1% uranyl acetate for 1 hour and dehydration was performed with graded ethanol series (70, 90, 96, and 100%).

The specimens were embedded in epon 812 (Epoxy Embedding Medium, Fluka [Buchs, Switzerland], Cat. No: 45345; DDSA, Merck, Cat. No: 1.12147; MNA,

Table 1. Scoring of Damage to Axonal Ultrastructure

Score	Degree of Damage	Description of Damage
1–	No damage	Mitochondria, microtubules, and microfilaments normal
1+	Low damage	Some vacuole and inclusions, some swelling in the mitochondria; and microtubule and microfilaments normal
2+	Mild damage	Large vacuoles, damaged external membrane and crista, formation of multilaminar structures, and swollen shape of mitochondria; and occasional abnormalities on the microtubules and microfilaments
3+	High damage	The same as in 2+ (mild damage), but in addition large areas of fragmented microtubules and microfilaments, or substantial absence of microtubules

Merck, Cat. No: 1.12251; DMP, Merck, Cat. No: 12388 [Merck Co., Whitehouse Station, NJ, USA]). Samples were trimmed and sectioned by using Leica MR 2,145 microtome (Heerbrugg, Switzerland) at 70 nanometer thickness and placed on copper grids, stained by 5% uranyl acetate and Reynold's lead citrate. The samples were then viewed and photographed under a JEM 1,011 transmission electron microscope (JEOL, Tokyo, Japan) at the Istanbul University, Institute for Experimental Medicine.

Sampling of axons from the sections was done at random positions across the sciatic nerve. No correlation was made in this study between the abnormalities observed and the distance from the axon in question to the electrode surface, although it is expected that electric field strength will vary substantially as a function of that distance.

RESULTS

The images from the electron microscopic study revealed an increased level of ultrastructural damage and disruption in the PRF-exposed axons (left side) as compared to the sham control axons (right side). Case examples from the numerous electron microscopy images are shown in Figures 2 to 7, and the results are summarized in Figure 8 and Tables 2 to 5. In these figures and tables, the standard classification of neurons is used. This classification is based on axon diameter and myelination. C-fibers axons have a diameter of 0.5 to 2 μm (micrometers) and are unmyelinated. A-delta fiber axons have a diameter of 2 to 5 μm and are myelinated. A-beta fibers have a diameter of 5 to 20 μm and are myelinated.

The images are all longitudinal slices because they show best any effects on axon membrane, mitochondria, and microtubules and microfilaments. The ordering of the images in Figures 2 to 7 have been selected in a progression of increasing damage and disruption as seen on the PRF-exposed axons and as quantified in the scoring shown in Table 1.

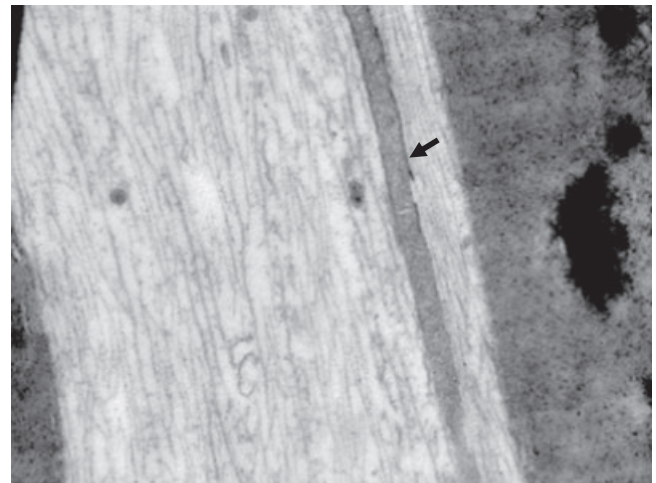


Figure 2. An electron micrograph ($\times 30,000$) from the sham control group (right side). The mitochondria (arrow) are intact and without defects, and the microtubules and microfilaments are also laminar and longitudinally well arranged. This is Score 1– in Table 1.

Figure 2 shows a typical electron micrograph through an axon in the sham control group (right side). The axoplasm contains well-aligned microtubule and microfilaments with no obvious abnormalities. The mitochondrion in the figure is well shaped and its membranes and crista are normal. This has an example of no damage, Score 1–, in Table 1.

Figure 3 shows a comparison of C-fiber electron micrographs from the PRF and the control groups. The control image on the right has normal microtubule, microfilaments, mitochondria, and axon membrane; Score 1– in Table 1. The image from the PRF group on the left has relatively normal patterns of microtubules and microfilaments, but has several distorted and swollen mitochondria that are invested with vacuoles and a cloudy white structure that invades the crista and possibly the inner and outer membranes of the mitochondria; this has Score 1+, low damage, from Table 1. In both cases the axonal membrane appears intact and normal.

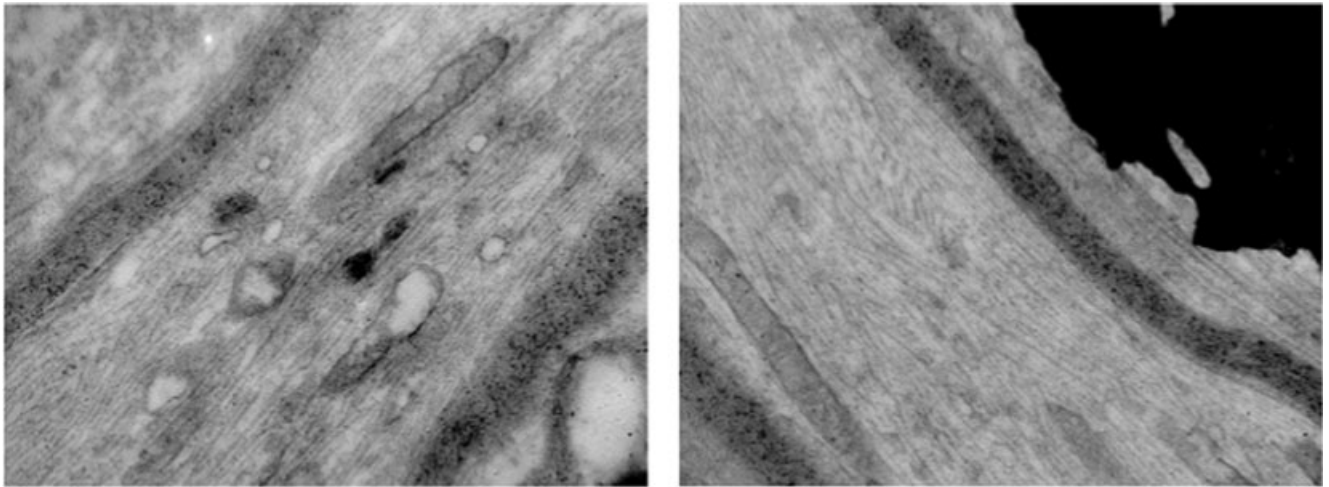


Figure 3. The right figure is an electron micrograph of a C-fiber ($\times 40,000$) from the sham control group (right side), which shows relatively normal microtubule and microfilament arrays and intact and normal mitochondria (Score 1–). The left figure shows an electron micrograph ($\times 30,000$) of a C-fiber from the pulsed radiofrequency group (left side) that has a normal pattern of microfilaments and microtubules, but has disrupted mitochondria (Score 1+, low damage).

Figure 4 shows two A-beta axons in the PRF group (left side), illustrating partial degree of ultrastructure disruption, classified as mild damage, Score 2+, in Table 1. The microtubules and microfilaments are distinct and mostly normal, although there are some small areas of nonlaminar disorganization that are not normal. Some mitochondria, but not all, show abnormal disruption. In the top image, some mitochondria have bloated whitish inclusions, although portions of their crista and inner membranes appear undisturbed. There are vesicles that are being transported and also appear to be normal. In the lower image, one mitochondrion has a swollen and distorted shape, and the inner white inclusion distorts the crista and membranes. A portion of the mitochondria's membrane may be compromised, although this may be difficult to distinguish from partial slice imaging.

Figure 5 shows images of two A-beta fibers in the PRF group (left side) that, again, show partial levels of abnormal ultrastructures. Here the microtubule and microfilaments are essentially normal. Vacuole inclusions appear inside the mitochondria, distorting them significantly and obliterating the crista. There are also multi laminar substances in the mitochondrial inner space. This is Score 2+ in Table 1.

Figure 6 shows images of two A-beta axons in the PRF group (left side) that have partial ultrastructural disruption. Microtubules and microfilaments appear normal, but the mitochondria are again swollen and disturbed. Portions of the mitochondria's membrane

may be breached by the whitish inclusion appearing in all of them. This was classified as Score 3+ in Table 1.

Figure 7 shows examples of severe ultrastructural damage observed in the PRF group (left side), scored as 3+, high damage. A significant difference from the previous figures is the widespread disruption and damage to the microtubules and microfilaments. This is in addition to the kind of damage to the mitochondria that is observed in Figures 3 to 6. Unlike the previous figures, the normal laminar pattern of microtubule and microfilament is missing. Instead, the entire axoplasm shows a broken and scattered field of short filaments. These filaments appear to be segments of microfilaments that have been broken and disarranged. The areas have essentially no microtubules in them, and only a few short segments of microtubules are visible at occasional locations throughout.

To quantify the comparison of the physical changes in the ultrastructure observed in the PRF-exposed group of axons (left side) and the sham control group of axons (right side), a scoring of the damage and disruption was established; this scoring scheme is summarized in Table 1 and illustrated in Figures 2 thorough 7. It is noted that damage to axons of the type shown in the figures could arise from sources other than the PRF exposure. For example, mechanical damage to axons and biochemical damage to cells such as anoxia during the preparation of the axon sample can potentially produce disruption of the type seen. Indeed, abnormalities of the types shown in Figures 2

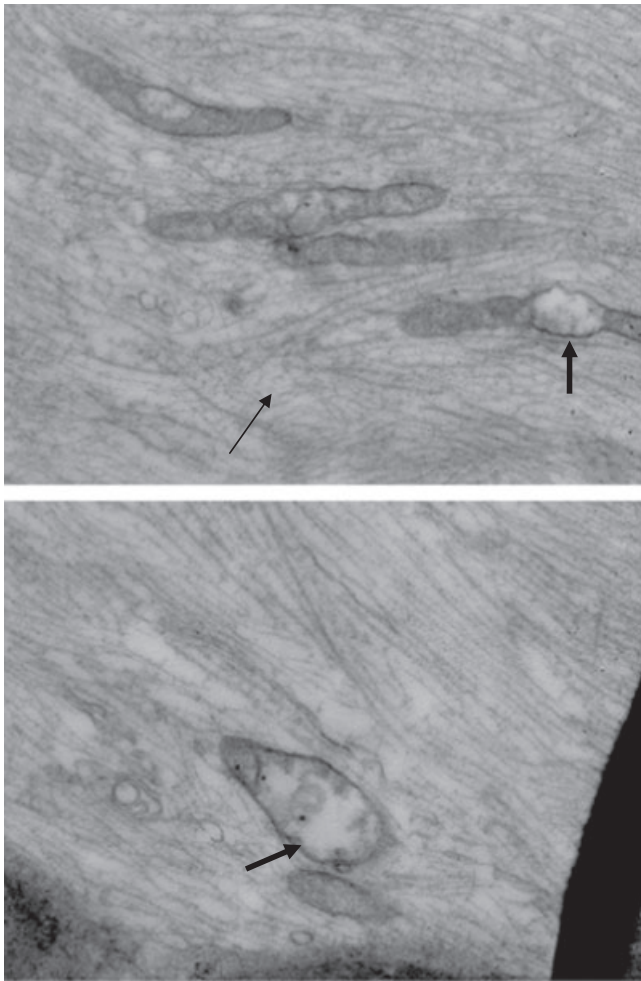


Figure 4. Electron microscopic images ($\times 40,000$) of an A-beta axons from the PRF group (left side) showing mild damage, Score 2+, of Table 1. In both images, abnormalities are not extreme, although there are some present. The microtubules and microfilaments are, for the most part, normal with distinct longitudinal directional patterns, with only small regions tending to be deviant (thin arrow in the top figure). Some of the mitochondria, but not all, have abnormal whitish inclusions that invest the crista and the inner membrane, and are swollen and misshapen (thick arrows). There is some evidence of partial slice imaging, which can account for fading of the membrane definition in places.

to 7 do occur to some degree in the control samples. Thus, the comparison of the PRF group and control group results based on this scoring is important to differentiate any PRF damages from damage from other spurious sources.

A number of axons were sampled from each of the PRF group (left side) and the sham control group (right side) to improve the statistical reliability of the scoring results. In all, there were 279 axons evaluated in the PRF group, which is the left side and designated as "L"

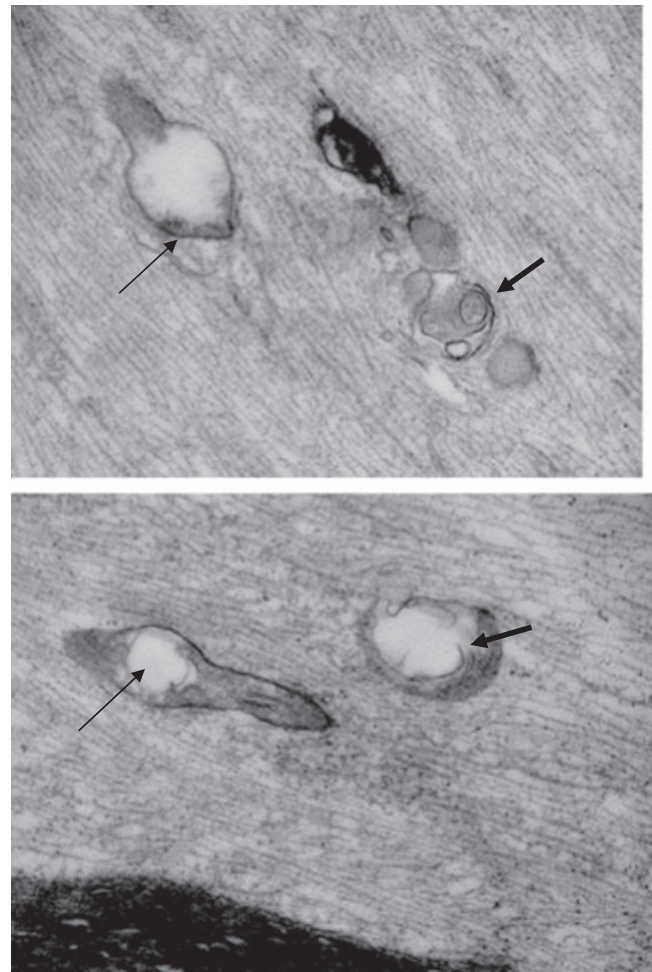


Figure 5. Electron micrographs ($\times 40,000$) of two separate A-beta axons in the pulsed radiofrequency group (left side) showing mild damage, Score 2+. In both images, the microtubule and microfilament arrays are normal. However, in the upper figure, the left mitochondria are bloated with white inclusions that invest the inner structure and possibly also the inner and outer membranes (thin arrow). The rightmost mitochondrion has degraded membranes and displays multilaminar substance formations (thick arrow). In the lower image, a vacuole is formed in the abnormally shaped mitochondria (thin arrow), and a multilaminar substance appears in the other mitochondria (thick arrow).

in the results in Tables 2 and 3 below; and there were 265 axons evaluated in the sham control group, which is the right side and designated as "R" in Tables 4 and 5.

DISCUSSION

The results in Figure 8 and Tables 2 to 5 show a difference in the effect on the PRF group compared to the sham control group. The PRF group shows substantially more ultrastructural damage in electron microscopy. The damage appears in only the structural elements

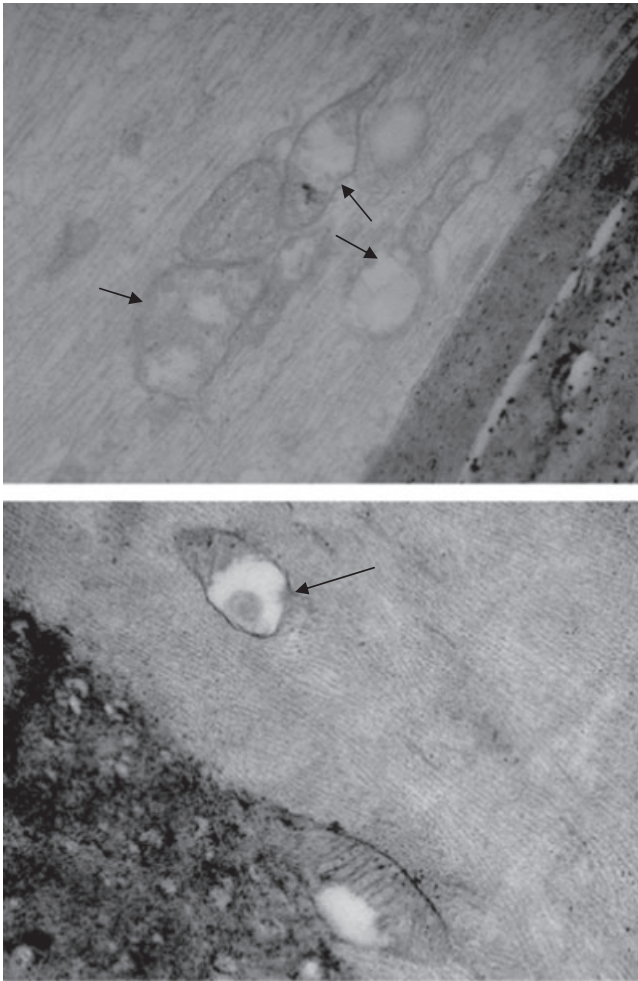


Figure 6. Electron micrographs ($\times 40,000$) in the PRF group (left side). Several mitochondria are abnormally swollen. White inclusions invade the crista and inner and outer membranes. The membranes appear abnormally defined and perhaps breached in places (arrows), although this could be an artifact of slicing and preparation. The microtubule and microfilament arrays are unremarkable. This is a Score 3+ in Table 1.

Table 2. PRF Group, Left Side (L): Number of Fibers

	Damage Score			
	1–	1+	2+	3+
A-beta	30	32	18	12
A-delta	28	22	25	16
C-fiber	10	18	23	34

PRF, pulsed radiofrequency.

within the axons, and no damage was evident to the outer axonal membrane in either group. It is notable however, that electron microscopy may not reveal microscopic changes in the axon membrane such as alteration of ion channels or pumps.

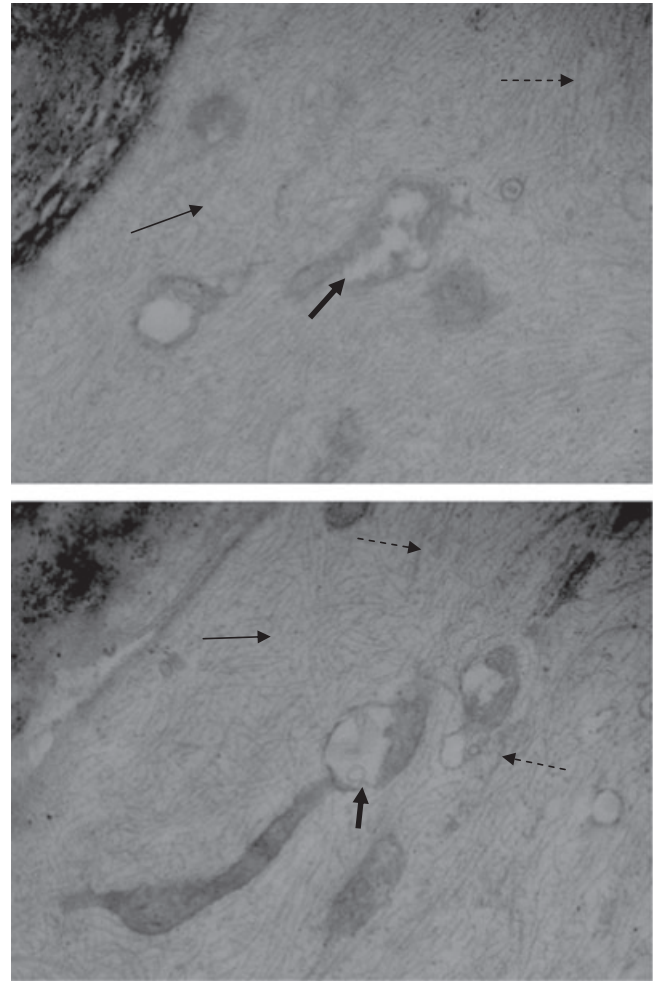


Figure 7. Electron micrographs ($\times 40,000$) of two different A-beta axons in the PRF group (left side), Score 3+, high damage. In both pictures the pattern of microtubules and microfilaments is seriously disrupted. Significant areas are filled with scattered short segments of non-longitudinal microfilament fragments and are devoid of any microtubules (thin arrows). Occasional microtubule fragments are evident (dashed arrows). Mitochondria are distorted and bloated, vacuoles and inclusions swell their inner space and crista, and their internal and exterior membranes appear damaged (thick arrows).

Table 3. PRF Group, Left Side (L): Percent of Fibers (%)

	Damage Score			
	1–	1+	2+	3+
A-beta	34	36	20	13
A-delta	31	24	27	18
C-fiber	12	21	27	40

PRF, pulsed radiofrequency.

Damage is seen in both the PRF and the control groups; however, the relative occurrence of damage is higher in the PRF group. It is possible that some damage, such as crushing injury or anoxia, may arise

from mechanical extraction and manipulation of the tissue, and the chemical preparation of samples for electron microscopy. However, by the relative comparison of the PRF vs. the control group, and by recruitment of a large enough sampling of neurons, these spurious sources of damage can be differentiated from PRF damage. Indeed, it appears that the PRF damage is statistically significant over the control group.

There is also a relatively greater degree of damage for smaller diameter fibers. The C-fibers (diameter 0.5 to

2 μm) show greater damage than the A-delta fibers (diameter 2 to 5 μm), and the A-delta fibers show a greater damage than the A-beta fibers (diameter 5 to 20 μm). It is known that the C-fibers and the A-delta fibers are the principal sensory nociceptors, and that the A-beta fibers are primarily related to touch and to non-pain-related sensations. Thus, the preferential effect of PRF on the C and A-delta fibers may suggest a connection to the pain relieving effect of PRF and its relative sparing of tactile sensory input.

Table 4. Sham Control Group, Right Side (R) Percent of Fibers (%)

	Damage Score			
	1–	1+	2+	3+
A-beta	62	14	7	8
A-delta	62	16	12	10
C-fiber	54	8	12	14

Table 5. Sham Control Group, Right Side (R) Percent of Fibers (%)

	Damage Score			
	1–	1+	2+	3+
A-beta	68	15	8	9
A-delta	62	16	12	10
C-fiber	61	9	14	16

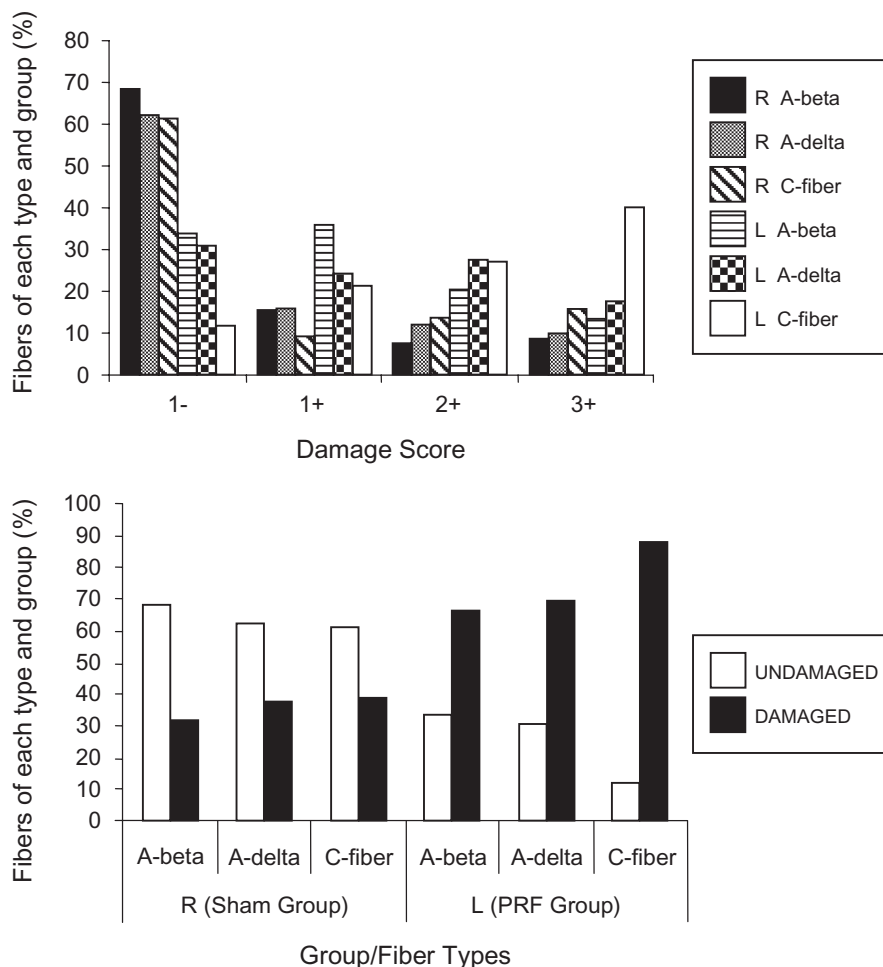


Figure 8. The upper histogram shows the percent of fibers of each type, within each group, that fall into the scoring categories as defined in Table 1. They are classified by different fiber diameters and by whether they are in the pulsed radiofrequency (PRF) group (L) or the sham group (R). The lower histogram shows the overall percentage of undamaged (1–) vs. damaged (1+, 2+, and 3+) fibers in each of the fiber types based on the damage score criteria of Table 1. A-beta fibers have diameter 4 to 20 μm , A-delta fibers have diameter 2 to 4 μm , and C-fibers have diameter < 2 μm .

Ultrastructural damage to sensory axons from PRF indicates that pulsatory PRF electric and current fields are penetrating the cell membrane, causing disruption to inner structures. The transmembrane potentials induced across the axonal membrane (neurolemma) by the PRF electric field have been calculated.³ At the PRF carrier RF in this experiment (500 kHz), the transmembrane potential partially shields the interior of the cell; however, there is also some cell penetration of the electric field, which is likely to have caused the ultrastructural damage seen here.

The magnitude of the PRF electric field that penetrates the axon has been calculated quantitatively.⁶ This calculation will be detailed in another publication, but a qualitative summary of its results is given here. The interior electric field is greater for larger diameter axons; however, it is reduced by the thickness of the cell membrane and myelin sheath. Thus, C-fibers, which have no myelin sheath, will have larger inner electric fields than A-delta fibers, which have myelin sheaths; and A-delta fibers will have higher interior fields than A-beta fibers because the former have thinner myelin sheaths than the latter. An exception is at the nodes of Ranvier, but this aspect has not been carefully studied here. Nevertheless, the progressive decrease in damage observed going from C-fibers to A-delta fibers, and from A-delta to A-beta fibers, is consistent with the predictions of the inner electric field calculations.⁶

The relationship of ultrastructural damage to antinociceptive effects of PRF remains to be clarified. Damage to mitochondria can have a profound effect on neuron function. The inner-axonal electric field produces a transmembrane potential on the inner and outer membranes of the mitochondria, and this too has been calculated.⁶ While its magnitude is not as great as the transmembrane potential on the axon's outer membrane, the mitochondria membranes are more fragile than the axonal membrane, and thus the mitochondria may be more sensitive to disruption. Mitochondria are the principal energy source of cells, producing ATP (adenosine triphosphate) in its inner matrix and inner membrane. ATP is essential for numerous functions, including ion channels and pumps, transport of vesicles on microtubules, and cell metabolism. Mitochondria are also critical to regulation and to production of numerous vital polypeptides and enzymes. Swollen mitochondria, as seen here, can cause blockage of all transport of vesicles along the microtubules,⁷ which is necessary to maintain cell function. The damage seen here could potentially inter-

rupt all of these functions and shut down the normal afferent signals that mediate pain.

The damage to microtubule and microfilament also can affect a neuron's ability to transmit signals. Microtubules are built from tubulin subunits, dimer proteins of alpha and beta types, which assemble longitudinally in a chain-like manner to form protofilaments. The protofilaments, in turn, aggregate laterally to form the microtubule. Microtubules, thus assembled, are cylindrical structures with diameter of about 24 nanometers and length that is variable, but typically in the micrometer (μm) range. The tubulin dimers as well as the microtubule assembly have an electrical polarity (a plus charge end and a minus charge end), which is essential for its basic functional purpose, namely, vesicle transport along the axon. Without this transport, the axon cannot replenish its vital elements and will not operate. A microtubule also has an overall net electrical charge. Thus, microtubules are charged and polar structures, and therefore are susceptible to electrical forces from inner-axonal electric fields produced by PRF.

The damage to microtubules and to microfilaments by PRF might theoretically arise from various mechanisms, some of which are mentioned here. Since they are charged objects, they might be directly disrupted by the inner-axonal PRF electric field. The microtubules are in a natural state of "dynamic instability," meaning that they are continuously shrinking and lengthening depending on factors such as concentration of tubulin and pH in the axoplasm. Any changes in these factors, such as that caused by damage to mitochondria, which control cell equilibrium, could cause a so-called "shrinkage catastrophe" and cause disappearance of microtubules. Microtubules maintain their integrity by continuously rebuilding themselves with tubulin subunits transported from the soma. This is powered by the mitochondria, and if that energy is cut off by damage to the mitochondria, the microtubule framework could disintegrate. Thus, microtubules and microfilaments can be affected either directly or indirectly by the PRF electric fields; that is, directly by either electric force acting on their charged structures, or indirectly by damage to the mitochondria, which in turn degrades the microtubules and microfilaments.

An estimate of relative energies and forces in the microtubule environment can provide some gauge of the likelihood of direct disruption of microtubules by the PRF fields. The dipole moments of tubulin dimers have been measured⁸ to be about 300 Debye per dimer, and for a 5- μm -long microtubule, this corresponds

to a dipole moment of $P_{\text{dip}} = 6.5 \times 10^3$ Debye (1 Debye = 3.3×10^{-30} coulomb-meters). The PRF electric field E outside the axon is about 50 KV/m maximum, assuming the axon is immediately against the PRF electrode. For an A-delta fiber, assuming a typical myelin thickness, the field inside the axon is about $E_{\text{in}} = 10$ KV/m. The maximum rotational energy for the dipole in that field is:

$$W_{\text{rot}} = P_{\text{dip}} E_{\text{in}} = 8 \times 10^{-20} \text{ Joules}$$

This can be compared to the thermal energy of agitation for a microtubule, which is:

$$W_{\text{therm}} = kT_0 = 4.2 \times 10^{-21} \text{ Joules}$$

where $k = 1.4 \times 10^{-23}$ Joules/K is Boltzmann's constant, and $T_0 \sim 300^\circ\text{K}$ (the absolute temperature scale is K, degrees Kelvin). Thus, the PRF rotational energy W_{rot} is 80 times the natural thermal energy W_{therm} , which means that the PRF electric field produces far greater rotational agitation of an intact microtubule than the thermal background noise.

The forces of motility of tubulin on microtubule provide another rough estimate. The motor protein kinesin provides the force to drive vesicles, other proteins, and tubulin substructures along the microtubule tracks in order to supply the vital elements of neurons function and to maintain the integrity of the microtubules themselves. There are studies on the magnitude of the longitudinal kinesin force,^{9,10} and give $F_{\text{long}} \sim 4$ to 8 pN (pico Newtons). An estimate of the lateral force on a microtubule, assuming a PRF electric field inside the axon of $E_{\text{in}} = 10$ KV/m and assuming an effective charge Q carried by the microtubule would be:

$$F_{\text{lat}} = QE_{\text{in}}$$

The measured values of Q depend on environment and measurement technique. One study¹¹ estimates $Q \sim 0.19 e^-$, where e^- is the elemental charge of 1.6×10^{-19} Coulombs, and this gives $F_{\text{lat}} = 2.5$ pN. Another study¹² gives $Q \sim 12 e^-$, which would result in $F_{\text{lat}} \sim 100$ pN. These values are comparable to F_{long} . Assuming that the lateral bonding force of kinesin to a microtubule is of the same order of magnitude as F_{long} , it is plausible that the lateral PRF force could separate microtubules from a track in the axon.

The complete dissociation energy of microtubules has been measured.¹³ This means breaking up the chain of tubulin dimers within the microtubule, and corresponds to the free energy of these bonds $\Delta G = 1.6 \times 10^{-20}$ Joules per dimer. An estimate of the rotational energy per

dimer from the PRF field would be the about the value of W_{rot} divided by the number of dimers in a microtubule. For a 5- μm -long microtubule, a dimer segment length of 8 nm (nanometer = $10^{-3} \mu\text{m}$) and the standard number of 13 dimers per dimer segment length means that the rotation energy per dimer is about $\Delta G/1600$. Thus, the PRF field is far too weak to break up the internal tubulin chain in an intact microtubule.

CONCLUSION

In this study, electron microscopy of sensory nociceptive axons shows physical evidence of ultrastructural damage following exposure to PRF. The mitochondria, microtubules, and microfilament all show various degrees of damage and disruption. The damage increases progressively from A-beta fibers to A-delta fibers to C-fibers. This is consistent with quantitative calculations of the strength of PRF electric field that penetrates the interior of the axons. It is also consistent with one clinically observed view that PRF may have a selectively greater effect on the smaller pain-carrying fibers (C-fiber and A-delta fibers), and a lesser affect on the larger A-beta neurons that mediate non-pain-related sensation. Estimates of the energies and forces expected from the PRF fields suggest that they are strong enough to cause the observed ultrastructural damage.

REFERENCES

1. Sluiter ME, Cosman ER, Rittman WJ, Van Kleef M. The effects of pulsed radiofrequency fields applied to the dorsal root ganglion—a preliminary report. *Pain Clin.* 1998;11:109–118.
2. Erdine S, Yucel A, Cimen A, Aydin S, Say A, Bilir A. Effects of pulsed versus conventional radiofrequency current on rabbit dorsal root ganglion morphology. *Eur J Pain.* 2005;9:251–256.
3. Cosman ER, Cosman ER. Electric and thermal field effects in tissue around radiofrequency electrodes. *Pain Med.* 2005;6:405–424.
4. Liliang PC, Lu K, Hsieh CH, Kao CY, Wang KW, Chen HJ. Pulsed radiofrequency of cervical medial branches for treatment of whiplash-related cervical zygapophysial joint pain. *Surg Neurol.* 2008;70:50–55.
5. Zimmermann M. Ethical guidelines for investigations of experimental pain in conscious animals. *Pain.* 1983;16:109–110.
6. Cosman ER, Cosman ER. *The physical effects of pulsed radiofrequency.* The Symposium on Invasive Procedures in Motion 2008; Nottwil, Switzerland, January 18–19, 2008.

7. Kaasik A, Safiulina D, Choubey V, Kuum M, Zharkovsky A, Veksler VJ. Mitochondrial swelling impairs the transport of organelles in cerebella granule neurons. *Biol Chem* 2007;282:32821–32826.
8. Nogales E, Wolf SG, Downing KH. Structure of the alpha beta tubulin dimer by electron microscopy. *Nature*. 1998;39:199–203.
9. Hunt AJ, Gittes F, Howard J. The force exerted by a single kinesin molecule against a viscous load. *Biophys J*. 1994;68:766–781.
10. Hall K, Cole D, Yeh Y, Baskin RJ. Kinesin force generation measured using a centrifuge microscope sperm-gliding motility assay. *Biophys J*. 1996;71:3467–3476.
11. Stracke R, Bohm KJ, Wollweber L, Tuszyński JA, Unger E. Analysis of the migration behavior of single microtubules in electric fields. *Biochem Biophys Res Commun*. 2002;293:602–609.
12. Martin GL, Van den Heuvel L, de Graaff MP, Dekkar C. Molecular sorting by electrical steering of microtubules in kinesin-coated channels. *Science*. 2006; 312:910–914.
13. Van Buren V, Odde DJ, Cassimeris L. Estimates of lateral and longitudinal bond energies within the microtubule lattice. *Proc Natl Acad Sci USA*. 2002;99:6035–6040.